CIVIL ENGINEERING JOURNAL

Article no. 9

THE CIVIL ENGINEERING JOURNAL 1-2026

CHARACTERISTICS OF INCINERATION BOTTOM ASH AS A POTENTIAL SUBSTITUTE FOR AGGREGATES AND CEMENT

Yongzhen Cheng, Weiye Mu, Baoliang Li, and Mengdi Zhou

Huaiyin Institute of Technology, Faculty of Architecture and Civil Engineering, Huai'an, No.89 Beijing North Road, China; chengyongzhen198@163.com

Received: 28.04.2025

Received in revised form: 15.09.2025

Accepted: 28.01.2026

ABSTRACT

The disposal of bottom ash from municipal solid waste incineration (MSWI) in landfills may lead to ecological contamination and inefficient land resources utilization. The investigation assessed whether MSWI bottom ash could serve as a substitute for sand and supplementary binder components in concrete production. Multiple analytical techniques were employed to characterize the MSWI bottom ash and its recycled powder. X-ray fluorescence (XRF) and laser particle size analysis were used to determine chemical composition and particle size distribution, respectively. Microscopic morphology and pore structure were examined with scanning electron microscopy (SEM) and nitrogen adsorption analysis. Phase composition was identified by X-ray diffraction (XRD), complemented with simultaneous thermal analysis (TG/DTG) and Fourier transform infrared (FTIR) spectroscopy. Results show that incineration bottom ash is coarse-grained and even exceeds the gradation range of Zone Ⅰ sand stipulated by the Chinese standard. Soaking and sieving treatment yields coarse bottom ash particles with clean surfaces, while fine bottom ash particles contain organic contaminants that are difficult to treat. The soaked bottom ash showed low Cl and SO_3 content, containing mainly quartz, calcite, gypsum, and hematite. The particles of bottom ash-derived powder are gravel-shaped, with pore sizes ranging from 1 nm to 70 nm and a high specific surface area. The pores are mainly mesopores, accounting for 73.83% of the total pore volume. BET measurements revealed a specific surface area six times greater than that of cement. Except for Cr, all heavy metal leaching levels comply with Chinese regulatory limits. MSWI bottom ash shows potential for partial replacement of natural sand or cement in construction applications.

KEYWORDS

Incineration bottom ash, Particle characteristics, Chemical components, Mineral composition, Pore structure

INTRODUCTION

The rapid growth of consumerism and industrial activities has significantly increased municipal solid waste generation. During the 2011-2023 period, medium-sized and large cities in China experienced consistent growth in municipal solid waste collection volumes, with the annual quantity peaking at 242.06 million tons in 2019 [1]. Current municipal solid waste management primarily utilizes three approaches: thermal treatment, land disposal, and biological decomposition. However, landfills have issues such as occupation of land resources and environmental pollution [2-4]. Incineration can achieve waste reduction and harmlessness, and the waste heat can be used for power generation [5, 6]. Therefore, large waste incineration plants have been built in many cities in

China. Moreover, the volume of waste incineration has increased rapidly annually, while landfill volume has decreased significantly.

Through incineration, the mass of domestic waste drops by roughly 70%, and simultaneously, a 90% reduction in volume is achieved. After the incineration process, two main types of residues are produced. Bottom ash, coming from the incinerator, and fly ash, obtained from the flue gas cleaning mechanism, together form these two main residues of incineration. Specifically, bottom ash accounts for about 80% of the total residue weight [7]. Bottom ash comprises an assortment of solid particles with disparate sizes, and these sizes range from fine particles to coarse fractions that exceed the gradation of Zone I sand specified in the national standard for construction sand of China (GB/T 14684), which corresponds to coarse-grained sand with a relatively large particle size distribution. Among its components are glassy substances, ceramic elements, mineral components, along with unburned materials, giving rise to a heterogeneous composition. Since bottom ash contains a certain amount of metals, electromagnetic and eddy-current separation is utilized to recover these valuable resources and further process the bottom ash. As a result, this separation technique effectively extracts specific metals from bottom ash.

Recent investigations have explored MSWI bottom ash as partial replacements for conventional aggregates in various construction applications, including cementitious composites, bituminous mixtures, and pavement foundations [8-11]. However, aggregates must comply with industry standards governing their structural, material, and functional characteristics [12, 13]. MSWI bottom ash-derived powder can also be used in concrete as a substitute for cement [14-16], overcoming the limitations in particle shape and gradation associated with its direct application as fine aggregate. While these studies confirm MSWI bottom ash application potential, most focus on feasibility rather than systematic characterization of key properties. This gap makes it difficult to guide targeted utilization of MSWI bottom ash.

The development of sustainable construction materials has driven growing interest in the utilization of industrial by-products. Notable examples include micro silica and fly ash, which are highly effective pozzolanic materials commonly used as partial substitutes for cement. Their role in enhancing the mechanical properties and durability of cementitious composites, specifically through reactions with calcium hydroxide to form additional C-S-H gel, is well established [17, 18]. However, the supply of these high-quality materials can be limited in certain regions. For instance, areas in China far from coal-fired power plants, which are a major source of fly ash, often face shortages of such materials. Furthermore, the diversity of waste streams calls for the exploration of a broader range of valorization options.

MSWI bottom ash represents a distinctly different type of material from the aforementioned micro silica and fly ash. Its potential value lies not in high pozzolanic reactivity, but rather in its dual functionality as a partial replacement for both fine aggregate and cementitious filler. In contrast to fly ash, which is largely pozzolanic, bottom ash consists of a heterogeneous combination of crystalline and amorphous phases. Therefore, instead of focusing on direct reactivity comparisons, this study provides a comprehensive characterization to evaluate its suitability for specific applications where high chemical reactivity is not the primary requirement. This approach helps diversify the range of waste-derived construction materials and reduces reliance on any single type of supplementary material.

This study systematically characterized MSWI bottom ash through multiple analytical techniques including XRF, XRD, SEM, TG/DTG, FTIR, and particle size analysis. The investigation focused on the following key aspects: particle composition, gradation characteristics, chemical components, mineral composition, and pore structure. The aim was to guide the efficient utilization of MSWI bottom ash as fine aggregate and cement replacement additive.

MATERIALS AND METHODS

Materials and treatment

The study utilized bottom ash from a municipal solid waste incineration plant in Suqian, China, with an annual processing capacity of 300,000 tons. Unsorted waste was directly fed into the incinerator, where combustion temperatures were maintained at 850-950℃ to ensure complete dioxin decomposition. The resulting bottom ash was water-quenched upon discharge from the grate, then processed through sequential metal recovery: electromagnetic separation for ferrous metals and eddy current separation for non-ferrous components.

The collected MSWI bottom ash contained trace organic components, such as plant roots, bark, and plastic fragments. To minimize potential interference from these materials with the reactivity of MSWI bottom ash, a water immersion treatment was applied. The bottom ash was fully submerged in water at a water-to-ash ratio of 2:1 and stirred thoroughly to ensure complete flotation of light organic components. After 24 hours of soaking, the water along with the floating organics was drained. The remaining solids were air-dried completely, then ground in a planetary ball mill at 350 r/min for 45 minutes. The milled product was sieved through a 200-mesh sieve with an aperture of 75 μm to remove oversized particles. This process produced a dark-gray powder with a maximum particle size of 75 μm.

P·II 52.5cement was used in this research, and its physical and mechanical properties met the requirements of Chinese standards [19].

Material properties analysis

The chemical components of the samples were tested by XRF (manufactured by Thermo Electron Corporation, USA; instrument model: ARL; detector resolution: MnKa resolution < 155 ev, CPS > 3000).

The D8-Discover X-ray diffraction was employed to analyze the mineral composition of samples. Test conditions: Cu tube, 40 kV, 36 mA, 10-90°, 4°/min.

The morphology of the samples was examined by SEM (manufactured by FEI Corporation, instrument model: Nova Nano SEM NPE218).

Thermogravimetric analysis of the samples was conducted by a simultaneous thermal analyzer (manufactured by NETZSCH; instrument model: DTG-60AH). The heating process was set within a range starting from the ambient temperature up to 1500 °C, at a constant increment rate of 10 °C per minute. Throughout the analysis, the samples were exposed to an inert atmosphere of nitrogen gas.

The infrared analysis of the samples was performed by FTIR (manufactured by Thermo Scientific, USA; instrument model: Nicolet iS10).

A laser particle size analyzer (manufactured by Microtrac, Inc.; instrument model: Microtrac S3500; dispersion medium: anhydrous ethanol) was utilized to determine the particle size distribution of the samples.

The adsorption/desorption curves of the samples were obtained by an Autosorb-IQ2 physical chemical adsorption analyzer.

Environmental impact assessment

The Chinese standard was applied to carry out the leaching toxicity test of MSWI bottom ash [18]. 20 grams of MSWI bottom ash-derived powder was weighed, oven-dried at 60 ℃, and then underwent a series of steps including sieving with a 5-mesh polypropylene sieve, grinding, and acid extraction treatment to obtain the extraction solution. Inductively coupled plasma mass spectrometry (ICP–MS) was employed to analyze the concentrations of heavy metals in the extraction solution.

RESULTS AND DISCUSSION

Physical properties

Particle and gradation characteristics of MSWI bottom ash

MSWI bottom ash is dark-gray in color, and its particle size and composition are similar to those of natural sand. Figure1 shows the particle size distribution curve of the MSWI bottom ash. The sampled bottom ash has a nominal maximum particle size of 4.75 mm. In compliance with the national standard for construction sand of China [13], when preparing cement concrete, sand from Zone II is recommended as the preferred choice. However, the bottom ash particles are coarse and even beyond the gradation range of Zone I sand specified in this standard. Since the coarse nature of bottom ash particles may undermine the workability and strength of concrete, when preparing concrete with bottom ash serving as fine aggregate, a sufficient amount of cement should be used to compensate for the low cohesive force of coarse particles, along with an increase in the sand ratio. Although increasing the cement content affects economic and environmental sustainability, the overall lifecycle assessment includes diverting MSWI bottom ash from landfills to reduce landfill pollution and conserving natural sand resources to alleviate resource scarcity. This assessment may still render this approach beneficial on a broader scale.

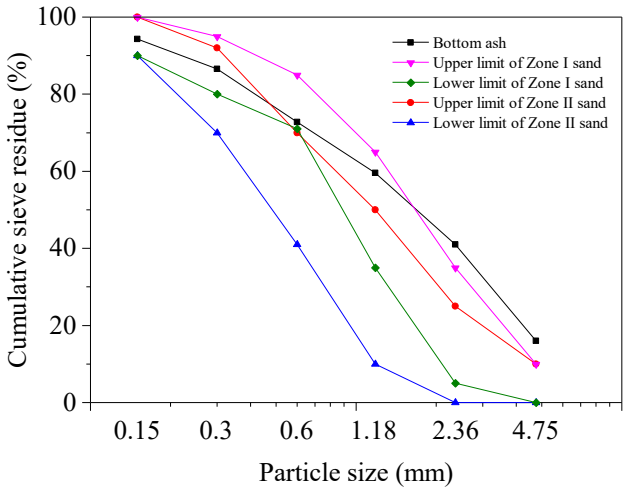

Fig. 1 - Gradation curve of MSWI bottom ash

The morphological features of MSWI bottom ash particles are illustrated in Figure 2. Morphological analysis reveals four predominant constituent components: quartz, glass fragments, ceramic shards, and slag. The composition further encompasses metallic oxides, especially iron-bearing particles.

Bulk analysis demonstrates that approximately 60% of bottom ash particles exhibit surface coatings comprising both fine-grained fractions and fused constituents. The fine particulate coatings develop on bottom ash surfaces through quenching-induced reactions during rapid water cooling [21]. During storage or transportation, bottom ash can be contaminated by the surrounding environment, resulting in the presence of some plant roots, bark and plastic products in it. Insufficient combustion of municipal solid waste can cause these pollutants to persist in bottom ash as well. In this research, water immersion effectively separated the majority of organic residues (including plant roots, skin debris, and plastic fragments) from the bottom ash. Consequently, the post-treated bottom ash exhibits clean particle surfaces without detectable fine particulate coatings. Additionally, MSWI bottom ash particles of varying sizes exhibit no substantial compositional differences. However, particle size influences phase distribution, with amorphous components (e.g., glass/ceramic fragments) showing enrichment in coarser fractions (>2.36 mm). Conversely, organic residues (plant

matter, plastics) predominantly occur in finer fractions sized 0.6–1.18 mm, and there is a notable increase in their content in even finer particles below 0.6 mm.

It is evident that glass and ceramic particles are enriched in the coarser fractions of bottom ash. Thus, the powder regenerated from coarser bottom ash contains more amorphous reactive phases with higher reactivity, which is more suitable for replacing cement as a supplementary cementitious material. The finer particles of the bottom ash contain more residual organic matter, which has a negative impact on cement hydration.

Morphological characteristics of MSWI bottom ash-derived powder

Figure 3 shows the SEM image of MSWI bottom ash-derived powder. The powder primarily consists of irregular, gravel-like particles, a key characteristic reported by Tang et al. [22]. Unlike fly ash, which contains spherical particles and exhibits water-reducing effects, the bottom ash powder lacks these properties. Additionally, small particles adhere to larger ones, forming agglomerates due to electrostatic interactions [23]. These morphological characteristics of MSWI bottom ash and its derived powder, combined with its gradation features, further distinguish its application scenarios from those of traditional supplementary cementitious materials.

Fig. 2 - Particles of MSWI bottom ash. (a) ⩾2.36 mm; (b) 0.6–1.18 mm

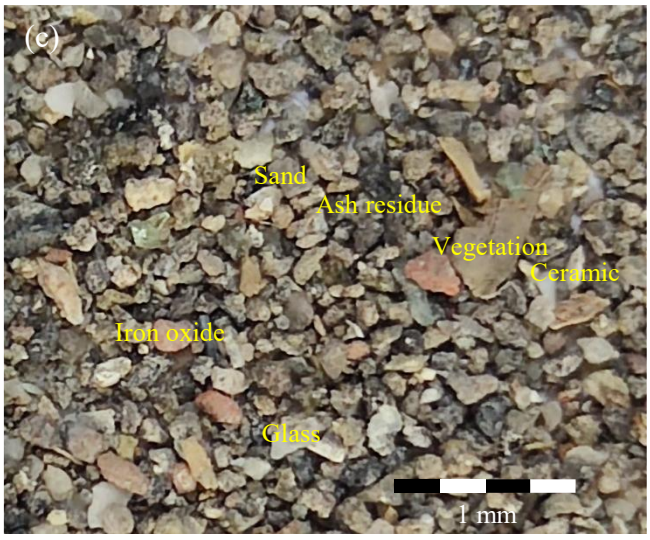

Fig. 2 - Particles of MSWI bottom ash.; (c) 0–0.6 mm

The morphological and gradation characteristics of MSWI bottom ash further clarify its application differences from traditional supplementary cementitious materials. For example, fly ash typically has spherical particles that improve concrete workability but require adjustment of sand ratio to compensate for poor gradation [24]; in contrast, the coarse-grained nature of bottom ash (exceeding Zone I sand) means it can partially replace natural sand in low-demand scenarios (e.g., pavement bases) without the need for additional “spherical particle modification”[10]. Meanwhile, compared with micro silica, which requires strict control of agglomeration due to fine particles [25], the gravel-like morphology of bottom ash-derived powder reduces agglomeration risk during mixing, which is more suitable for large-scale construction with simple mixing processes.

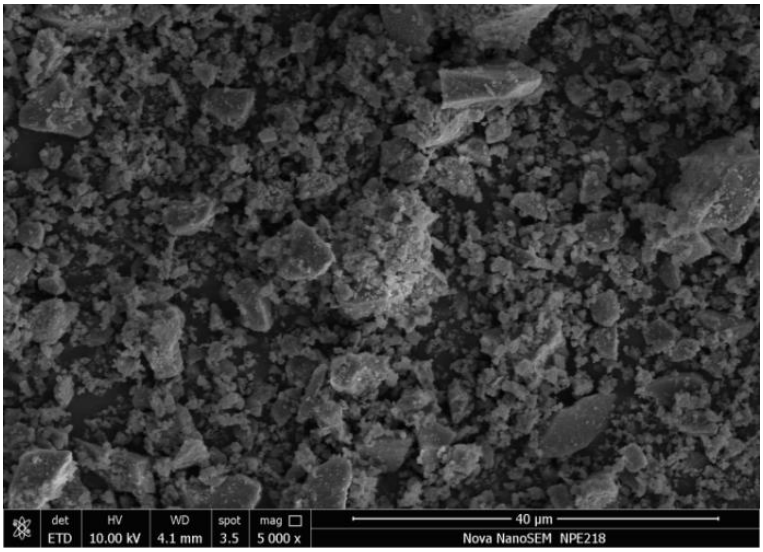

Fig. 3 - SEM image of MSWI bottom ash- derived powder. Scale bar: 40 µm.

Particle distribution of MSWI bottom ash-derived powder

Figure 4 illustrates the particle size distribution of the MSWI bottom ash-derived powder, with its granular characteristics summarized in Table 1. The powder particles are finer than cement particles, with all particles below 100 µm in size. This fineness results from high-speed milling with

sufficient duration, followed by sieving through a 75 μm mesh to remove large particles and impurities, yielding fine powder.

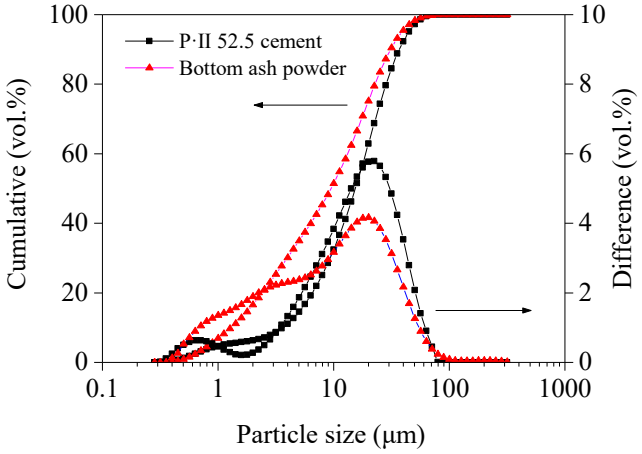

Fig. 4 - Particle size distribution of MSWI bottom ash-derived powder

Chemical components

Major oxides in both MSWI bottom ash and Portland cement (P·II 52.5) are quantified in Tab. 2. MSWI bottom ash exhibits a cement-like composition, primarily consisting of SiO_2, CaO, Al_2O_3, and Fe_2O_3. These four oxides collectively constitute over 85% of the bottom ash by mass. The bottom ash contains higher SiO_2 but lower CaO levels compared to cement. The contents of Al_2O_3 and Fe_2O_3 are 2 to 3 times greater than those in the cement. Na_2O, K_2O, and MgO are present in significant quantities in the bottom ash, representing typical alkali and alkaline earth oxides.

Tab. 1 - Particle size parameters of MSWI bottom ash-derived powder and cement

Particle size (μm)	P·Ⅱ 52.5 cement	Bottom ash-derived powder
d (0.1)	3.634	1.348
d (0.5)	15.367	10.267
d (0.9)	36.877	36.492
D (3, 2)	5.722	3.720
D (4, 3)	18.171	15.498

Tab. 2 - Major oxides in MSWI bottom ash and cement (%)

Chemical components	MgO	Na_2O	Al_2O_3	SiO_2	P_2O_5	K_2O	CaO
P·Ⅱ 52.5 cement	1.56	0.00	3.80	17.11	0.63	0.16	64.99
Bottom ash powder	2.49	3.87	9.22	49.45	2.31	2.29	19.37
Chemical components	TiO_2	MnO	Fe_2O_3	CuO	ZnO	Cl	SO_3
P·Ⅱ 52.5 cement	0.27	0.09	3.59	0.02	0.15	2.00	3.96
Chemical components	0.87	0.15	7.40	0.13	0.29	0.46	0.78

Cl (0.46 wt.%) and SO_3 (0.78 wt.%) concentrations in bottom ash are significantly below literature values. Garcia-Lodeiro et al. reported bottom ash typically contains 1.29% Cl and 2.54% SO_3 [26], while Vizcarra et al. found 2.3-3.8 wt.% Cl and 1.3-3.6 wt.% SO_3 [27]. Fine bottom ash

particles, like the fine particulate coatings, contain more chlorides and sulfates because of their large specific surface area. These particles form during water quenching and accumulate on the surface of coarse particles [28]. Saffarzadeh et al. showed that during water cooling and weathering, newly formed surface phases increase sites for chloride and sulfate absorption [29]. Immersing bottom ash in water causes dust on particle surfaces to separate and be carried away, reducing Cl and SO_3 levels in treated bottom ash.

The chemical composition shows that the sum of SiO_2, Al_2O_3, and Fe_2O_3 is about 62%, which is notably lower than the typical requirement of 70% for Class F fly ash as per ASTM C618 [30]. This quantitatively confirms the lower pozzolanic potential of MSWI bottom ash-derived powder compared to established supplementary cementitious materials. Consequently, its primary value in cement replacement applications may stem from its microfiller effect and its ability to provide nucleation sites for hydration products, rather than from significant pozzolanic contribution.

Mineral composition

XRD analysis (Figure 5) identifies quartz, calcite, gypsum, magnetite, and hematite as the dominant crystalline phases in MSWI bottom ash. Additionally, gehlenite, diopside and sodium feldspar are also detected in the bottom ash. Multiple active components, such as SiO_2, Al_2O_3, and CaO, exist in relatively high concentrations in MSWI bottom ash. However, MSWI bottom ash-derived powder lacks volcanic ash activity compared with fly ash [23]. This occurs since, rather than vitreous matter, most active components are present in stable crystal structures.

Stable crystalline phases (e.g., quartz, calcite) dominate over amorphous glassy phases, and these amorphous glassy phases are the primary source of reactivity in fly ash [31]. This further explains the limited pozzolanic activity observed in MSWI bottom ash-derived powder. This fundamental difference in phase composition between MSWI bottom ash and traditional supplementary cementitious materials (e.g., fly ash) underscores the need to identify applications that leverage its physical rather than chemical properties.

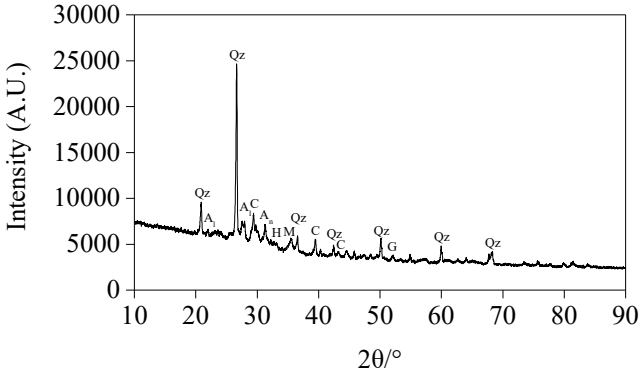

Fig. 5 - XRD pattern of MSWI bottom ash: Q: quartz (SiO_2); C: calcite ($CaCO_3$); G: gehlenite ($Ca_2Al_2SiO_7$); A_n: gypsum ($CaSO_4$); M: magnetite (Fe_3O_4); H: hematite (Fe_2O_3); D: diopside ($CaMgSi_2O_6$); A_l: sodium feldspar ($NaAlSi_3O_8$)

Figure 6 presents the FTIR spectrum of MSWI bottom ash, with key absorption bands assigned based on literature [32-36]: At 3420 cm^{-1}, the vibrational band corresponds to the stretching vibration of H-OH groups in free water. This band links to the adsorbed water and crystalline water of gypsum present in bottom ash; The 2520 cm^{-1} band corresponds to the vibrational mode of carbonate; The peak at 2360 cm^{-1} shows the vibrational mode of HPO_3^{-2}, indicating a small amount of phosphate in the bottom ash; The 1650 cm^{-1} absorption is characteristic of C=O asymmetric stretching, indicating surface-bound aromatic compounds, carboxylic acids, amino groups, or lipids; The peaks at 1450 cm^{-1}, 876 cm^{-1} and 730 cm^{-1} correspond to the asymmetric stretching vibration, out-of-plane bending vibration, and in-plane bending vibration of CO_3^{-2}; The antisymmetric stretching

band at 1040 cm^{-1} and the symmetric stretching band at 780 cm^{-1} are due to the presence of quartz; The peak at 600 cm^{-1} corresponds to the vibrational mode of sulfate.

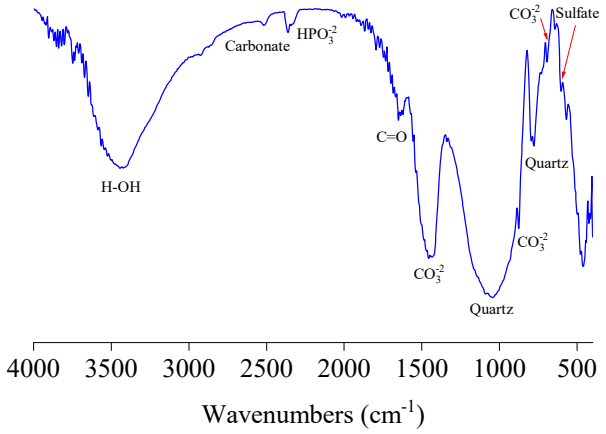

Fig. 6 - FTIR spectrum of MSWI bottom ash

Figure 7 displays TG/DTG curves for MSWI bottom ash. Based on these curves, bottom ash pyrolysis progresses through four sequential stages. Stage I: The bottom ash sample is heated to 114°C and experiences a mass loss of 0.85%. Evaporation of adsorbed water causes this mass reduction. Stage II: At 504°C and 570°C, a 3.34% weight loss occurs as hydrated silicate, chlorate, and other minerals undergo dehydration. Stage III: At 676°C, a weight loss of 2.32% corresponds to the decomposition of $CaCO_3$. Stage IV: At 1022°C, a weight loss of 0.7% corresponds to the decomposition of gypsum.

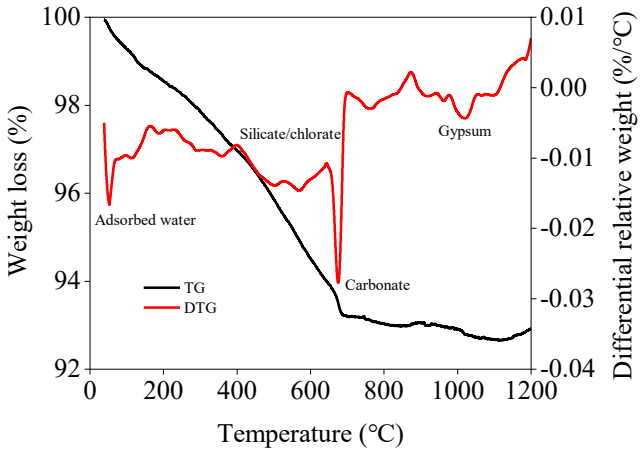

Fig. 7 - TG/DTG curves of MSWI bottom ash

The thermal decomposition of $CaCO_3$ (676 ℃, 2.32% mass loss) indicates two key implications: first, bottom ash may release CO_2 during cement hydration (a factor to consider in high-temperature scenarios like mass concrete) and a potential mass loss upon heating (critical for high-temperature applications); second, the presence of SiO_2 provides a basis for secondary hydration [37]. Beyond the contribution of SiO_2, the carbonate from $CaCO_3$ decomposition also plays a role in regulating the hydration process. More importantly, the presence of carbonate can affect the hydration process by interacting with calcium aluminate phases, potentially leading to the formation of carboaluminate phases, and these phases can densify the microstructure.

Pore structure of MSWI bottom ash-derived powder

Adsorption/desorption curves

The adsorption/desorption isotherm curves of MSWI bottom ash-derived powder are shown in Figure 8. According to the classification of gas physisorption isotherms [38], MSWI bottom ash-derived powder exhibits a Type II-like adsorption profile, though with less pronounced inflection at low relative pressures. These isotherms arise from unimpeded monolayer-to-multilayer adsorption under elevated pressure conditions, with distinct features as described below: For the condition where P/P0≤0.05, nitrogen adsorption enters its first stage. This initial stage is defined as the process of monolayer adsorption. When $0.05<P/P_0\leq0.9$, the adsorption isotherm rises slowly and multilayer adsorption begins to occur, corresponding to the second stage of nitrogen adsorption. Once P/P0 exceeds 0.9, capillary coalescence of nitrogen occurs. This leads to a rapid upward trend in the adsorption isotherm.

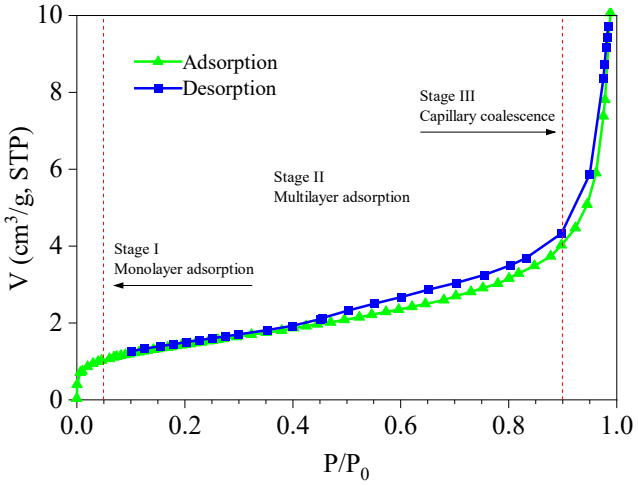

Fig. 8 - Adsorption/desorption isotherm curves of MSWI bottom ash-derived powder

Hysteretic behavior arises from non-overlapping adsorption-desorption isotherms. This hysteretic phenomenon varies significantly across systems, primarily governed by pore density, structural morphology, and size dispersity. Per IUPAC guidelines [38], MSWI bottom ash-derived powder exhibits combined H3-H4 type hysteresis, indicative of flexible lamellar particle aggregates containing interconnected macropores with partial capillary condensation.

Pore size distribution

The cumulative volume and differential size distribution of pores in MSWI bottom ash-derived powder are illustrated in Figure 9. Pores in porous materials can be categorized into three types: macroporous (＞50 nm), mesoporous (2–50 nm) and microporous (＜2 nm). As shown by the distribution curves, pores in MSWI bottom ash-derived powder vary significantly in size (1-70 nm). The average pore size, determined from cumulative pore volume analysis, measures 11.58 nm. Macropores represent 17.63% of the pore volume, while mesopores dominate at 73.83%, followed by micropores at 8.54%.

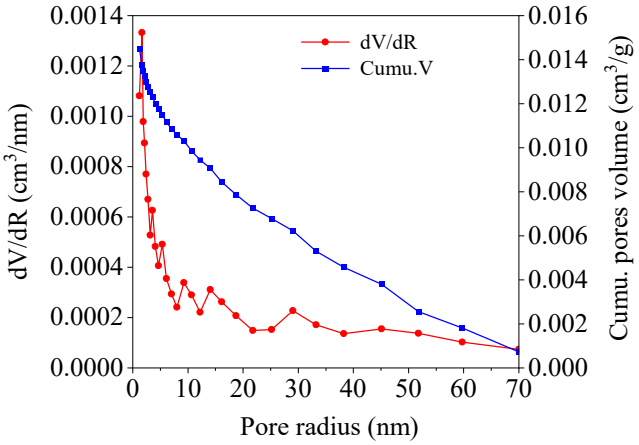

Fig. 9 - Cumulative pore volume and differential pore size distribution of MSWI bottom ash-derived powder

The BET surface area of MSWI bottom ash-derived powder measures 5.38 m²/g, showing good agreement with previous findings. As reported by Marieta et al. [36], one MSWI bottom ash-derived powder sample exhibited a specific surface area of 7.43 m²/g, while the other registered 5.30 m²/g. The BET method provides more reliable specific surface area measurements by eliminating the need for particle shape assumptions or semi-empirical corrections Marieta [39]. There is a significant correlation between the reactivity of powder and its particle size [40]. Powder fineness indicated by specific surface area directly correlates with the reactivity potential of bottom ash. Furthermore, adsorption capacity shows direct dependence on specific surface area in micro powders. Compared to ordinary Portland cement, the MSWI bottom ash-derived powder under study exhibits a significantly larger specific surface area. Li et al. [35] reported 0.88 m²/g for P·II 52.5 cement, merely one-fifth the specific surface area measured in MSWI bottom ash-derived powder.

Although this study primarily focuses on the fundamental characterization of municipal solid waste incineration (MSWI) bottom ash, its intrinsic properties, including particle size distribution, morphology, chemical and mineral composition, and pore structure, directly influence its potential mechanical performance in cementitious systems. Tang et al. [22] examined how the physicochemical properties of treated MSWI bottom ash and its cement replacement ratio affect the strength of cement-sand mortars. The results indicated that reducing the organic matter content mitigates its inhibitory effect on cement hydration, while the thermal decomposition of calcite ($CaCO_3$) generates new reactive phases, thereby enhancing the reactivity of the recycled ash. Finer ash powder was found to contribute to a denser mortar microstructure, leading to improved strength. The combined physical filling effect and favorable chemical composition, predominantly SiO_2–CaO–Al_2O_3, enable recycled MSWI bottom ash powder to serve effectively as a 30% cement replacement in low-strength mortars [41]. Physically, the mesoporous structure of the milled ash facilitates pore filling; chemically, its composition supports slow pozzolanic reactions and secondary hydration.

It is also important to note that, as with many single supplementary cementitious materials, the replacement ratio of MSWI bottom ash must be carefully optimized. Li et al. [23] reported that replacing 30% of cement with MSWI bottom ash resulted in an approximately 26% decrease in the 28-day compressive strength of mortar, which aligns with the replacement ratio of 30% or less as recommended in the environmental risk assessment section of this study. These findings suggest that MSWI bottom ash is most suitable for partial cement replacement in medium and low strength applications, such as non-structural concrete and pavement subgrades. It provides a sustainable alternative to conventional high-performance materials like microsilica or blended supplementary cementitious materials.

Environmental impact assessment

GB 5085.3 [20] mandates that leachate from hazardous waste must keep hazardous component concentrations below prescribed thresholds to ensure environmental and human health protection. The leaching behavior of MSWI bottom ash was characterized by ICP-MS, with quantitative results detailed in Tab. 3. The leaching amounts of all metals except Cr are lower than the limits set by Chinese legislation.

It is critical to emphasize that this standard leaching test was performed on the raw bottom ash powder in isolation. In practical cementitious applications, two key factors mitigate the environmental risk: (1) the incorporation rate of alternative materials like bottom ash is typically limited to below 30% [23], and (2) the encapsulation effect of the cement matrix is widely documented to significantly immobilize heavy metals, drastically reducing their leachability [42]. This encapsulation phenomenon represents the primary mechanism for risk reduction in real-world scenarios. Therefore, while the elevated Cr leaching from the raw powder is noted, its environmental impact in a solidified cementitious system is anticipated to be substantially lower. A comprehensive investigation into the long-term leaching behavior from engineered mortar/concrete composites remains a valuable focus for future studies.

Tab. 3 - The leaching properties of MSWI bottom ash-derived powder

Metals	As	Cr	Cd	Hg	Ni	Pb	Zn
Bottom ash powder (mg/L)	0.3943	8.7173	0.0005	0.0003	3.7926	1.9682	9.1731
Limits (mg/L)	5	5	1	0.1	5	5	100

CONCLUSION

(1) The gradation of MSWI bottom ash resembles that of Zone Ⅰ sand. In addition, bottom ash particles of varying sizes exhibit no significant disparity in their constituents. Coarse bottom ash fractions are enriched with ceramic and glass particulates, whereas finer fractions accumulate more residual plant matter and synthetic contaminants from incomplete combustion or external sources.

(2) MSWI bottom ash features a chemical composition similar to that of cement, with SiO_2-CaO-Al_2O_3-Fe_2O_3 being the main components. Compared to cement, MSWI bottom ash contains a relatively higher proportion of SiO_2 and a lower proportion of CaO, while mineralogical characterization reveals quartz, calcite, gypsum and hematite as major constituents.

(3) MSWI bottom ash-derived powder exhibits distinctive physical characteristics, featuring fine granulometry, high porosity, and a large surface area. Particle morphology analysis reveals gravel-like irregularity, with fine particulate matter adhering to coarser particle surfaces.

(4) The hybrid H3/H4 hysteresis loop observed in the Type II isotherm reflects the complex pore structure of MSWI bottom ash-derived powder, where mesopores constitute the primary void space within the broadly distributed pore network.

REFERENCES

[1] National Bureau of Statistics of China, 2011-2023. China Statistical Yearbook. China Statistics Press, Beijing.

[2] Shu S., Zhu W., Xu H.Q., Wang S.W., Fan X.H., Wu S.L., Shi J.Y., Song J., 2019. Effect of the leachate head on the key pollutant indicator in a municipal solid waste landfill barrier system. Journal of Environmental Management, vol. 239, p. 262-270.

[3] Peng W., Pivato A., Wang T.F., 2019. Stabilization of solid digestate and nitrogen removal from mature leachate in landfill simulation bioreactors packed with aged refuse. Journal of Environmental Management, vol. 232, p. 957-963.

[4] Sekhohola-Dlamini L., Tekere M., 2020. Microbiology of municipal solid waste landfills: a review of

microbial dynamics and ecological influences in waste bioprocessing. Biodegradation, vol. 31, no. 1-2, p. 1-21.
[5] Li M., Xiang J., Hu S., Sun L.S., Su S., Li P.S., Sun X.X., 2004. Characterization of solid residues from municipal solid waste incinerator. Fuel, vol. 83, p. 1397-1405.
[6] Sisani F., Maalouf A., Di Maria F., 2022. Environmental and energy performances of the Italian municipal solid waste incineration system in a life cycle perspective. Waste Management & Research, vol. 40, no. 2, p. 218-226.
[7] Chimenos J.M., Segarra M., Fernandez M.A., Espiell F., 1999. Characterization of the bottom ash in municipal solid waste incinerator. Journal of Hazardous Materials, vol. 64, no. 3, p. 211-222.
[8] Grazulyte J., Vaitkus A., Šernas O., Žalimienė L., 2022. The impact of MSWI bottom ash as aggregate on concrete mechanical performance. International Journal of Pavement Engineering, vol. 23, no. 9, p. 2903-2911.
[9] Singh A., Zhou Y.Y., Gupta V., Sharma R., 2022. Sustainable use of different size fractions of municipal solid waste incinerator bottom ash and recycled fine aggregates in cement mortar. Case Studies in Construction Materials, vol. 17, e01434.
[10] Suddeepong A., Buritatum A., Dasdawan S., Horpibulsuk S., Yaowarat T., Hoy M., Arulrajah A., 2023. Mechanical performance of porous asphalt concrete incorporating bottom ash as fine aggregate. Journal of Materials in Civil Engineering, vol. 35, no. 6, 04023129.
[11] Lu J.G., Yang X.L., Lai Y., Wan X.S., Gao J.J., Wang Y.D., Tan L.L., Deng F., 2024. Utilization of municipal solid waste incinerator bottom ash (MSWIBA) in concrete as partial replacement of fine aggregate. Construction and Building Materials, vol. 414, 134918.
[12] JTG F40. Technical Specifications for Construction of Highway Asphalt Pavement. 2004.
[13] JGJ 52. Standard for Technical Requirements and Test Method of Sand and Crushed Stone. 2006.
[14] Maldonado-Alameda A., Giro-Paloma J., Svobodova-Sedlackova A., Formosa J., Chimenos J.M., 2020. Municipal solid waste incineration bottom ash as alkali-activated cement precursor depending on particle size. Journal of Cleaner Production, vol. 242, 118443.
[15] Cheng L., Jin H.S., Wu Y.K., Ren Y.R., Liu J., Xing F., 2024. Influence of municipal solid waste incineration bottom ash particle size on cement hydration and performance. Construction and Building Materials, vol. 432, 136516.
[16] Song H., Fan S.J., Che J.H., Yao J.W., Lee Y.G., 2024. Physical & mechanical properties of pervious concrete incorporating municipal solid waste incineration bottom ash. Journal of Building Engineering, vol. 96, 110599.
[17] Szcześniak, A., Siwiński, J., Stolarski, A., Piekarczuk, A., Nasiłowska, B., 2024. The influence of the addition of microsilica and fly ash on the properties of ultra-high-performance concretes. Materials, vol. 18, no. 1, 28.
[18] Khankhaje, E., Kim, T., Jang, H., Kim, C.S., Kim, J., Rafieizonooz, M., 2023. Properties of pervious concrete incorporating fly ash as partial replacement of cement: a review. Developments in the Built Environment, vol. 14, 100130.
[19] GB 175. Common Portland Cement. 2007.
[20] GB 5085.3. Identification Standards for Hazardous Wastes-Identification for Extraction Toxicity. 2007.
[21] Yang S., Saffarzadeh A., Shimaoka T., Kawano T., 2014. Existence of Cl in municipal solid waste incineration bottom ash and dechlorination effect of thermal treatment. Journal of Hazardous Materials, vol. 267, p. 214-220.
[22] Tang P., Florea M.V.A., Spiesz P., Brouwers H.J.H., 2016. Application of thermally activated municipal solid waste incineration (MSWI) bottom ash fines as binder substitute. Cement and Concrete Composites, vol. 70, p. 194-205.
[23] Li X.G., Lv Y., Ma B.G., Chen Q.B., Yin X.B., Jian S.W., 2012. Utilization of municipal solid waste incineration bottom ash in blended cement. Journal of Cleaner Production, vol. 32, p. 96-100.
[24] Mishra, S.K., Upadhyay, B., Das, B.B., 2025. 3D printing aspects of fly ash and GGBS admixed binary and ternary blended cementitious mortar. European Journal of Environmental and Civil Engineering. https://doi.org/10.1080/19648189.2025.2521381
[25] Akmalaiuly, K., Berdikul, N., Pundienė, I., Pranckevičienė, J., 2023. The effect of mechanical activation of fly ash on cement-based materials hydration and hardened state properties. Materials, vol. 16, no. 8, 2959.
[26] Garcia-Lodeiro I., Carcelen-Taboada V., Fernández-Jiménez A., Palomo A., 2016. Manufacture of hybrid cements with fly ash and bottom ash from a municipal solid waste incinerator. Construction and Building Materials, vol. 105, p. 218-226.
[27] Vizcarra G.O.C., Casagrande M.D., da Motta L.M.G., 2014. Applicability of Municipal Solid Waste Incineration Ash on Base Layers of Pavements. Journal of Materials in Civil Engineering, vol. 26, no. 6,

06014005.
[28] Chen C.H., Chiou I.J., 2007. Distribution of chloride ion in MSWI bottom ash and de-chlorination performance. Journal of Hazardous Materials, vol. 148, p. 346-352.
[29] Saffarzadeh A., Shimaoka T., Wei Y.M., Gardner K.H., Musselman C.N., 2011. Impacts of natural weathering on the transformation/neoformation processes in landfilled MSWI bottom ash: a geoenvironmental perspective. Waste Management, vol. 31, no. 12, p. 2440-2454.
[30] ASTM C618-23, 2023. Standard specification for coal fly ash and raw or calcined natural pozzolan for use in concrete. ASTM International.
[31] Wei, G.Q., Dong, B.Q., Fang, G.H., Wang, Y.S., 2023. Understanding reactive amorphous phases of fly ash through the acidolysis. Cement and Concrete Composites, vol. 140, 105102.
[32] Martinez-Ramirez S., 1999. Influence of SO2 deposition on cement mortar hydration. Cement and Concrete Research, vol. 29, p. 107-111.
[33] Ismail I., Bernal S.A., Provis J.L., Nicolas R.S., Hamdan S., van Deventer J.S.J., 2014. Modification of phase evolution in alkali-activated blast furnace slag by the incorporation of fly ash. Cement and Concrete Composites, vol. 45, p. 125-135.
[34] Xu Y.F., Fu Y., Xia W., Zhang D., An D., Qian G.R., 2018. Municipal solid waste incineration (MSWI) fly ash washing pretreatment by biochemical effluent of landfill leachate: a potential substitute for water. Environmental Technology, vol. 39, no. 15, p. 1949-1954.
[35] Li B.L., Wang Y.H., Peng D., Yang L., Zhang Y.M., 2019. Composition and Suitable Application of Electric Furnace Ferronickel Slag Sand and Ferronickel Slag Powder. Materials Reports, vol. 33, no. 11, p. 3752-3756.
[36] Marieta C., Guerrero A., Leon I., 2021. Municipal solid waste incineration fly ash to produce eco-friendly binders for sustainable building construction. Waste Management, vol. 120, p. 114-124.
[37] McDonald, L.J., Carballo-Meilan, M.A., Chacartegui, R., Afzal, W., 2022. The physicochemical properties of Portland cement blended with calcium carbonate with different morphologies as a supplementary cementitious material. Journal of Cleaner Production, vol. 338, 130309.
[38] Thommes M., Kaneko K., Neimark A.V., Olivier J.P., Rodriguez-Reinoso F., Rouquerol J., Sing K.S.W., 2015. Physisorption of gases, with special reference to the evaluation of surface area and pore size distribution (IUPAC Technical Report). Pure and Applied Chemistry, vol. 87, no. 9-10, p. 1051-1069.
[39] Mantellato S., Palacios M., Flatt R.J., 2015. Reliable specific surface area measurements on anhydrous cements. Cement and Concrete Research, vol. 67, p. 286-291.
[40] Chen C.G., Sun C.J., Gau S.H., Wu C.W., Chen Y.L., 2013. The effects of the mechanical-chemical stabilization process for municipal solid waste incinerator fly ash on the chemical reactions in cement paste. Waste Management, vol. 33, p. 858-865.
[41] Zhang, S.P., Ghouleh, Z., He, Z., Hu, L.L., Shao, Y.X., 2021. Use of municipal solid waste incineration bottom ash as a supplementary cementitious material in dry-cast concrete. Construction and Building Materials, vol. 266, 120890.
[42] Wang, D.Q., Wang, Q., 2022. Clarifying and quantifying the immobilization capacity of cement pastes on heavy metals. Cement and Concrete Research, vol. 161, 106945.